Suppression of First-wall Interaction in Negative Triangularity Plasmas on TCV

W. Han[1], N. Offeddu[2], T. Golfinopoulos[1], C. Theiler[2], C. K. Tsui[3], J. A. Boedo[3], E. S. Marmar[1] and the TCV team[2]‡

[1]MIT Plasma Science and Fusion Center, Cambridge, Massachusetts 02139, USA
[2]École Polytechnique Fédérale de Lausanne (EPFL), Swiss Plasma Center (SPC), CH-1015 Lausanne, Switzerland
[3]University of California-San Diego, La Jolla, California 92093, USA

E-mail: harryhan@mit.edu

Abstract. Magnetically confined fusion plasmas with negative triangularity (δ) exhibit greater L-mode confinement than with positive δ. Recent experiments in the TCV and DIII-D tokamaks have correlated the confinement improvement to a reduction of fluctuations within the plasma core. We report on fluctuation measurements in the Scrape-Off Layer (SOL) for $-0.61 < \delta < +0.64$ in limited and diverted ohmic L-mode plasmas; these reveal a strong reduction in SOL fluctuation amplitudes at $\delta \lesssim -0.25$, and, surprisingly, an almost full suppression of plasma interaction with the main-chamber first-wall, which could have important implications for the prospects of using negative δ plasmas as a reactor solution. An exploration of several physical mechanisms suggests that a reduced connection length—intrinsic to negative δ plasmas—plays a critical role in the origin of this phenomenon.

‡ See Coda *et al* 2019 (https://doi.org/10.1088/1741-4326/ab25cb) for the TCV team.

In tokamak fusion devices, core plasma shapes with negative triangularity, δ, are known to exhibit a substantial increase in L-mode energy confinement compared to the usual positive δ, D-shaped plasmas [1]. This is accompanied by reductions in the fluctuation levels of the core electron temperature [2, 3] and density [4, 3]. Operation with negative δ has recently been extended to high values of plasma β [3]. Moreover, plasmas of negative δ are promising candidates for a future fusion reactor as part of a "power-handling-first" philosophy [5].

The sign and strength of triangularity may also have a large effect on plasma edge dynamics and power and particle exhaust properties, but relatively little is presently known about such effects. Experiments with lower single-null configurations revealed a considerable reduction of the scrape-off layer (SOL) power fall-off length (λ_q) with decreasing upper triangularity [6] and first-principle turbulence simulations for limited configurations predict a transition in the SOL turbulence regime for sufficiently negative δ that would reduce turbulence amplitude and SOL pressure scale lengths [7]. In this letter, we report on detailed plasma edge/SOL measurements across a range of plasma triangularities from $+0.64$ to -0.61, revealing a strong reduction of far-SOL fluctuations for sufficiently negative values of δ. This results in a near-complete suppression of plasma interaction with the main-chamber first-wall for $\delta \lesssim -0.25$. This is robustly observed across a wide range of densities in both inner-wall-limited and diverted plasmas and may strongly alleviate concerns of high levels of first-wall heat and particle loads expected in conventional, positive δ reactors [8, 9]. This reduction in first-wall plasma interaction is accompanied by a steepening of the ion saturation current profile in the SOL and a reduction in the radial velocities of turbulent structures. These changes are found to correlate well with a reduction in connection length, characteristic of negative δ plasmas.

1. Experimental setup

The reported experiments were performed in ohmic-heated L-mode plasmas on the Tokamak à Configuration Variable (TCV) [10] at a toroidal field $B_T = 1.4$ T and plasma current $I_p = 230$ kA. Both the inner-wall-limited with $-0.37 < \delta < +0.38$ and diverted discharges with $\delta = -0.61, +0.64$ had a fixed elongation, $\kappa \sim 1.4$. Plasma densities were varied from 1.7×10^{19} to 5.8×10^{19} m^{-3}, corresponding to Greenwald fractions of 0.13–0.42. In this set of ohmic plasmas, no significant difference in core confinement was observed between positive and negative δ cases, consistent with results shown by [1].

High-resolution fluctuation measurements near the outer mid-plane were obtained from wall-mounted Langmuir probes (LP), a reciprocating probe (RP), and gas puff imaging (GPI), with their respective locations illustrated in Fig. 1. In particular, four of the TCV wall LPs [11], located at the low-field side of the GPI views, are used to monitor first-wall interactions. They were configured to locally measure the ion saturation current density (J_{sat}) at 200 kHz. The RP is located nearby and measures J_{sat} and floating potential (V_f) during a fast radial scan, providing plasma fluctuation profiles together with electron temperature (T_e), density (n_e), and plasma potential (Φ) profiles [12].

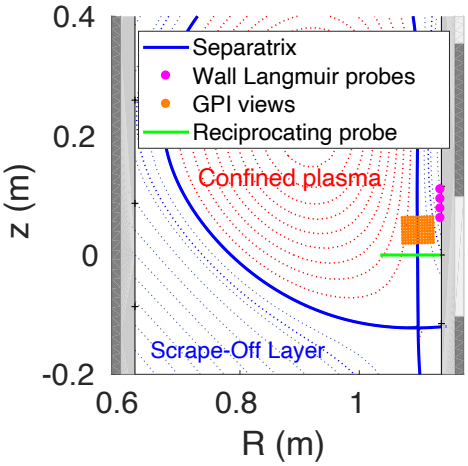

Figure 1. Poloidal cross-section of a diverted, negative triangularity plasma with the locations of wall Langmuir probes, GPI views, and reciprocating probe indicated.

Gas puff imaging (GPI) measures the spatially-resolved edge/SOL fluctuations by imaging neutral atomic spectral-line emission from a local gas puff [13]. We commissioned the GPI diagnostic on TCV in December 2018. A rectangular 10x12 array of fibers, viewing the gas puff at the outboard mid-plane along lines-of-sight that are approximately aligned with the local B-field, is coupled to avalanche photo-diode (APD) detectors through D_α (656 nm) or He I (587 nm) filters, with the signals digitized at 2 MHz. The views have 4.3 mm spot spacing and 3.9 mm spot size in the focal plane at the location of the gas puff. The data presented here are from deuterium gas puffs in conjunction with D_α filters. The helicity of the plasmas was adjusted to align as closely as possible the magnetic field with the lines of sight of GPI, which have a 5 degree pitch angle. We note that the pitch angle of the magnetic field at the measurement location is ~ 9 degrees, and varies weakly as a function of δ.

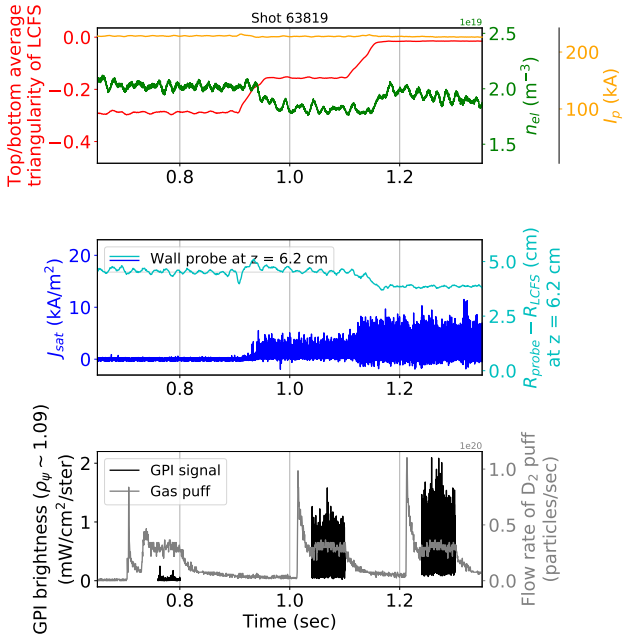

Figure 2. Time traces of the triangularity (red), the line-averaged density of the plasma (green), the plasma current (yellow), the saturation current of the wall probe (blue) and its radial location relative to the LCFS (cyan), the GPI brightness in the SOL (black), and the flow rate of D_2 puff (gray). Triangularity is scanned in steps.

2. Results

Fig. 2 shows, for an inner-wall-limited plasma, time traces of plasma current, density, and triangularity, together with the saturation current density from one of the outer wall LPs and the GPI brightness in the SOL. The GPI brightness and the wall probe J_{sat} show very low fluctuations in the SOL for $\delta = -0.3$. High-intermittency fluctuation signals, characteristic for the tokamak SOL, are recovered only when triangularity is increased to $\delta = -0.16, -0.01$.

The two-dimensional GPI measurements in Fig. 3 clearly show this drastic change. The left column shows poloidal cross-sections of three limited plasmas with $\delta = +0.38, -0.15, -0.37$ and two diverted plasmas with $\delta = +0.64, -0.61$. The orange and magenta dots, and the green line are, again, the location of the GPI views, the wall probes, and the reciprocating probe, respectively. The right column of Fig. 3 shows the fluctuation RMS (the root-mean-squared fluctuation about the mean, i.e. the standard deviation of the brightness) for the GPI views, evaluated over a 10 ms time window. The Last Closed Flux Surface (LCFS) and the separatrix locations are drawn as a red and a blue line, respectively. For the $\delta = -0.37, -0.61$ plasmas, a strong drop in the fluctuation RMS is apparent in the outer region of the SOL, that is not reproduced for the $\delta = +0.64, +0.38, -0.15$ plasmas,

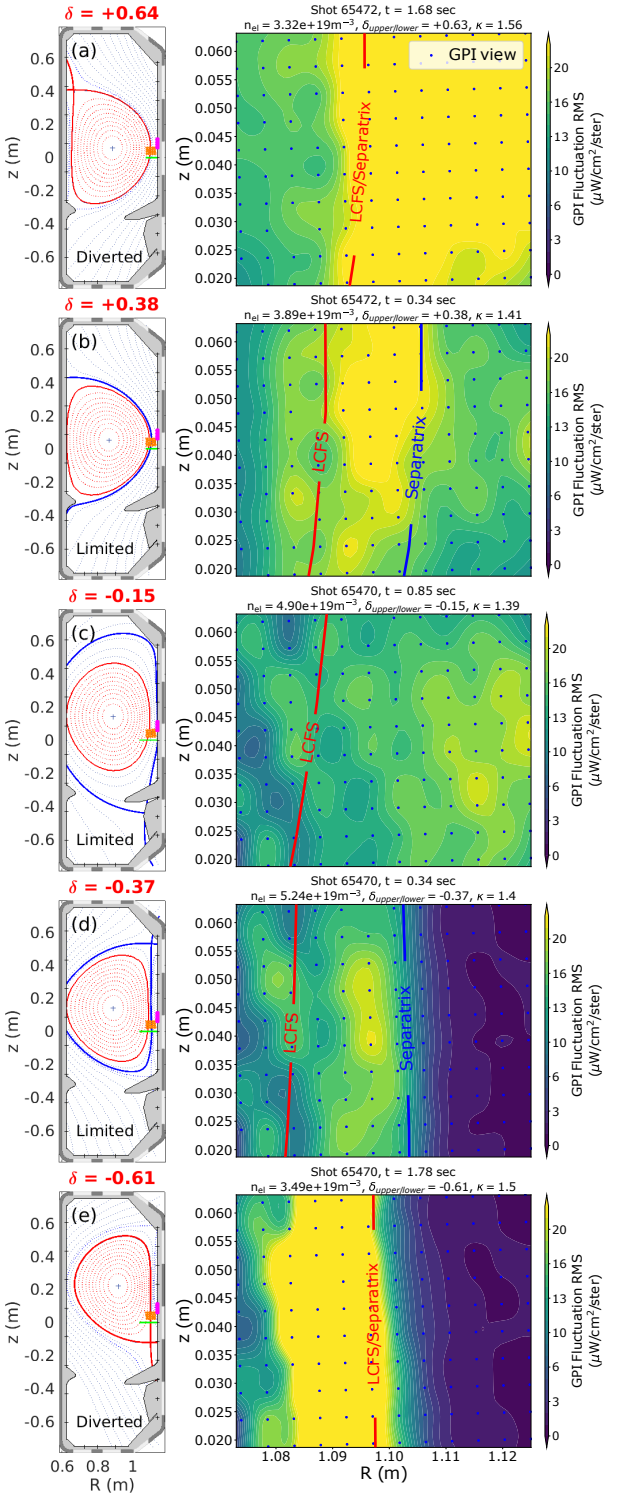

Figure 3. Poloidal cross sections of the flux surfaces of plasmas (three limited: $\delta = +0.38, -0.15, -0.37$, two diverted: $\delta = +0.64$, $\delta = -0.61$) (left) and the corresponding fluctuation RMS ($\mu W/cm^2/ster$) over a 10 ms window of the brightness measured from the GPI views (right).

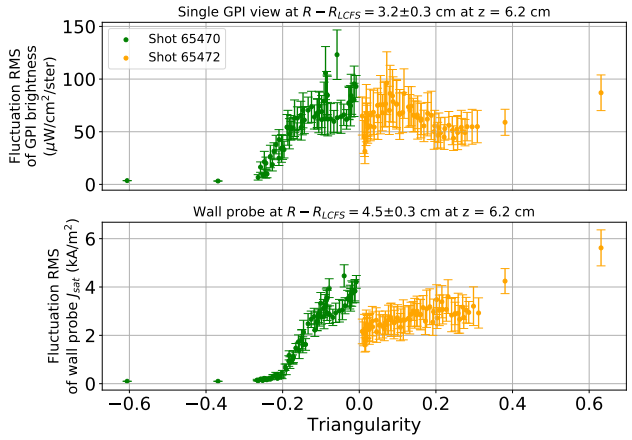

Figure 4. Fluctuation RMS of GPI brightness in the SOL (top) and fluctuation RMS of the wall probe J_{sat} (bottom) as a function of δ. These are inner-wall-limited plasmas, except $\delta = +0.64$ and -0.61 which are diverted cases.

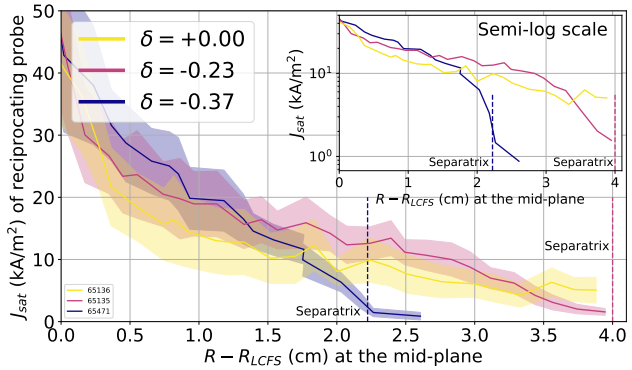

Figure 5. Radial profiles of J_{sat} and its fluctuation RMS (indicated by the shaded region), as measured with the reciprocating probe for different values of δ. The inset shows a semi-log plot of the radial J_{sat} profiles.

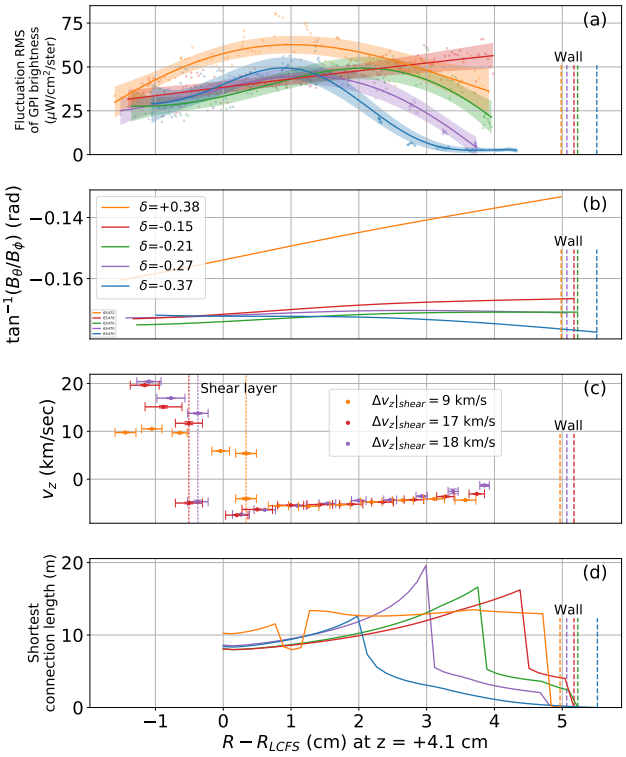

Figure 6. (a) Fluctuation RMS of GPI brightness, (b) pitch angle ($\tan^{-1}(B_\theta/B_\phi)$), (c) vertical velocity (v_z) of fluctuations (from dispersion relation of each column of GPI views), and (d) shortest connection length to the wall, as a function of $R - R_{LCFS}$ for inner-wall-limited plasmas with $\delta = +0.38$, -0.15, -0.21, -0.27, -0.37. v_z in (c) is scaled by the sign of the direction of the electron diamagnetic drift.

regardless of being limited or diverted. This reduction of the fluctuations in the outer SOL are observed robustly over the entire density range explored, from 1.7×10^{19} to 5.8×10^{19} m^{-3}.

The abruptness of this transition in SOL fluctuation amplitudes is apparent in Fig. 4, from the fluctuation RMS of the GPI brightness at a fixed view ($R - R_{LCFS} \sim 3.2$ cm) and from the fluctuation RMS of the wall probe J_{sat} at $R - R_{LCFS} \sim 4.5$ cm during continuous and discrete triangularity scans. Both GPI and the wall probe show fluctuations that sharply increase for δ above ~ -0.2, then saturate above ~ -0.1.

Radial profiles of ion saturation current density (J_{sat}) measurements from the reciprocating probe confirm the GPI and wall probe observations. Beyond a radial position of $R - R_{LCFS} \sim 1.7$ cm, the fluctuation RMS, shown by the shaded region in Fig. 5, drops substantially for sufficiently negative δ. What is also apparent from Fig. 5 is a clear transition in the time-averaged J_{sat} profile for $\delta = -0.37$, showing a narrower SOL width with little plasma remaining in the far-SOL ($R - R_{LCFS} > 2.3$ cm). A similar trend appears in the radial profile of the fluctuation RMS of GPI brightness in Fig. 6 (a), where the SOL fluctuation RMS becomes suppressed as δ is scanned from +0.38 to −0.37.

3. Discussion

We now discuss the possible origin of this strong dependence of SOL dynamics and first-wall interaction on triangularity. Changes in turbulence and scale lengths could result from a change in the turbulence regime and/or E×B shear-flow turbulence suppression [14]. Simulations of inner-wall-limited plasmas [7] found that, for sufficiently high plasma elongation and negative δ, the typically dominant Resistive Ballooning Modes (RBMs) become stabilized, narrowing the SOL width and transitioning to turbulence dominated by Resistive Drift Waves (RDWs). RBM stabilization was intuitively explained in this work by increased

magnetic field pitch near the outer mid-plane, resulting in field lines spending less time in the bad curvature region where RBMs are destabilized. To probe this explanation, Fig. 6 (b) plots the radial profiles of outer mid-plane magnetic field pitch of inner-wall-limited plasmas over a range of δ. The pitch angle indeed increases as δ varies from -0.15 to -0.37, which is the range where the change in SOL fluctuation RMS is observed in Fig. 6 (a). However, this pitch change of < 0.01 radian is considerably smaller than that between $\delta = +0.38$ and $\delta = -0.15$, where similar fluctuation amplitudes are apparent in Fig. 6 (a). More direct evidence of RBM stabilization can be deduced by calculating the cross-phase between the plasma density (n_e) and the poloidal electric field (E_θ) fluctuations [7]. RP data of plasmas for three triangularities ($\delta = -0.22, +0.01, +0.22$) [15] reveals a change in the n_e-E_θ cross-phase between $\delta = +0.22$ and $+0.01$. However, similar analysis for lower δ values did not show significant changes in cross-phase, in particular around $\delta \sim -0.25$, where the reduction in first-wall interaction is observed. From this evidence, we conclude that RBM stabilization is not responsible for the sharp reduction in far-SOL fluctuations as δ decreases below ~ -0.25.

The E×B shear may be implicated if it changes as a function of δ, as stronger shear can diminish turbulent eddies, suppressing turbulence. Fig. 6 (c) shows the vertical velocity of fluctuations (v_z) estimated from a linear-fit of the ω-k_z spectrum evaluated for each column of GPI views (i.e. the phase velocity). This inverts at the shear layer ($R-R_{LCFS} \sim -0.5$ cm for $\delta = -0.27, -0.15$ and $R - R_{LCFS} \sim +0.3$ cm for $\delta = +0.38$). The change in v_z at the shear layer is similar for $\delta = -0.27$, -0.15 ($\Delta v_z|_{shear} \sim 18$, 17 km/s) and smaller for $\delta = +0.38$ ($\Delta v_z|_{shear} \sim 9$ km/s). Analysis of the entire data set reveals an abrupt change in $\Delta v_z|_{shear}$ only at $\delta \sim +0.3$. This suggests that there is no significant change in the strength of the shear for triangularities between -0.27 and -0.15, whereas Fig. 6 (a) shows suppressed fluctuation RMS in the SOL as δ is scanned across this range.

Having found no evidence for the turbulence regime change or poloidal flow shear as explanations for the suppression of first-wall interaction, we note a striking difference in connection length as δ becomes sufficiently negative. Fig. 6 (d) shows radial profiles of the shortest magnetic field line length from the mid-height of the GPI views to the wall, over a range of triangularities. For negative δ cases, beyond a certain radius, the connection length decreases substantially. This is due to the X-point in the low-field side SOL, which directs the field lines more towards the outer-wall, as seen in Fig. 3 (d) and (e). As δ becomes more negative, this field line deviation to the outer-wall occurs closer to the LCFS. Interestingly, this behavior correlates very well with the radial location in the SOL beyond which the fluctuation amplitude drops, as apparent from a comparison with Fig. 6 (a). This could be due to the filaments or blobs that dominate radial transport in the far-SOL region becoming "discharged" by the short connection length, with a reduction in radial transport resulting from the loss of polarization. Changes in connection length and/or strong magnetic shear that occurs near X-points have already been documented to substantially reduce the radial velocities of plasma blobs [8, 16, 17]. In the present case, for negative δ and outside the separatrix, we expect the blobs to be in the sheath-limited regime, where their radial velocity does depend on the connection length. Indeed, a rough estimate gives a normalized blob size $\hat{a} \sim 1.3$–2.5 and a collisionality parameter $\Lambda \sim 0.2$ [18], where we used the typical blob sizes in these plasmas of 0.5–1.0 cm, $L_\parallel \sim 4$ m, $R \sim 1.1$ m, $B \sim 1.4$ T, $n_e \sim 0.3 \times 10^{19}$ m^{-3}, and assuming $T_e \sim T_i \sim 10$ eV, at a position outside the separatrix. This hypothesis is strengthened by determining the radial velocity of blobs through Conditional Average Sampling (CAS), as depicted in Fig. 7. Here, a spatial and temporal average of coherent turbulent structures (in the present case blobs) is performed, at a selected location, using a trigger threshold condition [19]. This can suppress random noise and fluctuations and highlight any statistical spatial and temporal evolution of the detected structures. The radial velocity can then be deduced from the 2D, CAS blob motion for a range of radial positions in the SOL, as shown in Fig. 7. $\delta = -0.01$, -0.16, -0.29 cases were chosen to span the critical value of $\delta \sim -0.25$. For $\delta = -0.29$, radial velocities in the SOL are strongly reduced for $R - R_{LCFS} > 2$ cm, by approximately a factor of four compared with the $\delta = -0.16$ and -0.01 cases, while

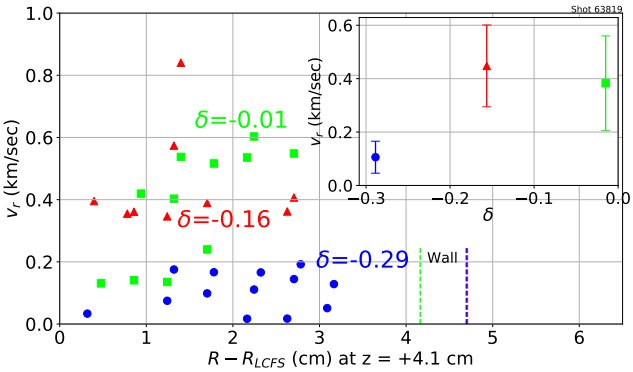

Figure 7. Radial profiles of the radial velocity of plasma blobs (v_r) calculated by CAS for inner-wall-limited plasmas with $\delta = -0.01$, -0.16, and -0.29. The means and the standard deviations of v_r as a function of δ are shown in the inset.

vertical propagation in the SOL is nearly unaffected by δ, as shown in Fig. 6 (c). These observations support a shorter connection length as the cause of the reduced first-wall interaction, although magnetic shear in the vicinity of the nearby X-point may also play a role. Clearly, whether these results extrapolate to future, larger devices is currently an open question. However, we note that short connection lengths are a generic feature of negative triangularity configurations, both for limited plasmas sufficiently far out in the SOL (beyond the separatrix) as well as for diverted plasmas. This connection length reduction is due to the shorter poloidal span between the outer mid-plane and the X-point, as well as a higher pitch angle, especially in the vicinity of the X-points. This, in turn, results from the larger major radius of the X-point and outer SOL, where the toroidal field is lower.

4. Conclusions and remarks

The strong reduction in main-chamber first-wall plasma interaction at sufficiently negative triangularity reported in this letter strengthens the prospects of negative triangularity plasmas as a potential reactor solution. This foresees operation in negative triangularity L-mode plasmas with H-mode-like confinement and a concomitant absence of harmful Edge-Localized Modes (ELMs). SOL widths, although likely narrower than in positive triangularity L-mode plasmas, as suggested by [6] and the present work, may be comparable to typical SOL widths in conventional H-mode plasmas. Heat and particle exhaust in a dedicated divertor chamber, foreseen for this purpose, will then not necessarily be more challenging than for positive δ, also considering the ease to place the divertor target at a large major radius. The reported strong suppression of main-chamber first-wall interaction will then constitute a key benefit of negative δ, alleviating the risks associated with first-wall erosion and main-chamber recycling [8, 9].

Acknowledgments

The authors thank J. L. Terry, B. P. Duval, and A. Merle for invaluable suggestions. The support from US Department of Energy, Fusion Energy Sciences, awards DE-SC0014264, DE-SC0020327, and DE-SC0010529, are gratefully acknowledged. Also, this work was supported in part by the Swiss National Science Foundation. This work has been carried out within the framework of the EUROfusion Consortium and has received funding from the Euratom research and training programme 2014–2018 and 2019–2020 under grant agreement No 633053. The views and opinions expressed herein do not necessarily reflect those of the European Commission.

References

[1] Camenen Y, Pochelon A, Behn R, Bottino A, Bortolon A, Coda S, Karpushov A, Sauter O and Zhuang G (TCV Team) 2007 *Nuclear Fusion* **47** 510–516 URL https://doi.org/10.1088%2F0029-5515%2F47%2F7%2F002

[2] Fontana M, Porte L, Coda S and Sauter O (TCV Team) 2017 *Nuclear Fusion* **58** 024002 URL https://doi.org/10.1088%2F1741-4326%2Faa98f4

[3] Austin M E, Marinoni A, Walker M L, Brookman M W, deGrassie J S, Hyatt A W, McKee G R, Petty C C, Rhodes T L, Smith S P, Sung C, Thome K E and Turnbull A D 2019 *Phys. Rev. Lett.* **122**(11) 115001 URL https://link.aps.org/doi/10.1103/PhysRevLett.122.115001

[4] Huang Z and Coda S (TCV Team) 2018 *Plasma Physics and Controlled Fusion* **61** 014021 URL https://doi.org/10.1088%2F1361-6587%2Faadb59

[5] Kikuchi M, Takizuka T, Medvedev S, Ando T, Chen D, Li J, Austin M, Sauter O, Villard L, Merle A, Fontana M, Kishimoto Y and Imadera K 2019 *Nuclear Fusion* **59** 056017 URL https://doi.org/10.1088%2F1741-4326%2Fab076d

[6] Faitsch M, Maurizio R, Gallo A, Coda S, Eich T, Labit B, Merle A, Reimerdes H, Sieglin B and Theiler C (Eurofusion MST1 Team and TCV Team) 2018 *Plasma Physics and Controlled Fusion* **60** 045010 URL https://doi.org/10.1088%2F1361-6587%2Faaaef7

[7] Riva F, Lanti E, Jolliet S and Ricci P 2017 *Plasma Physics and Controlled Fusion* **59** 035001 URL https://doi.org/10.1088%2F1361-6587%2Faa5322

[8] Carralero D, Manz P, Aho-Mantila L, Birkenmeier G, Brix M, Groth M, Müller H W, Stroth U, Vianello N and Wolfrum E (ASDEX Upgrade Team and JET Contributors and EUROfusion MST1 Team) 2015 *Phys. Rev. Lett.* **115**(21) 215002 URL https://link.aps.org/doi/10.1103/PhysRevLett.115.215002

[9] Vianello N, Carralero D, Tsui C, Naulin V, Agostini M, Cziegler I, Labit B, Theiler C, Wolfrum E, Aguiam D *et al.* 2019 *Nuclear Fusion* **60** 016001 URL https://doi.org/10.1088%2F1741-4326%2Fab423e

[10] Coda S, Agostini M, Albanese R *et al.* 2019 *Nuclear Fusion* **59** 112023 URL https://doi.org/10.1088%2F1741-4326%2Fab25cb

[11] De Oliveira H, Marmillod P, Theiler C, Chavan R, Février O, Labit B, Lavanchy P, Marlétaz B and Pitts R A 2019 *Review of Scientific Instruments* **90** 083502 URL https://doi.org/10.1063/1.5108876

[12] Tsui C K, Boedo J A, Halpern F D, Loizu J, Nespoli F, Horacek J, Labit B, Morales J, Reimerdes H, Ricci P, Theiler C, Coda S, Duval B P and Furno I 2017 *Physics of Plasmas* **24** 062508 URL https://doi.org/10.1063/1.4985075

[13] Zweben S J, Terry J L, Stotler D P and Maqueda R J 2017 *Review of Scientific Instruments* **88** 041101 URL https://doi.org/10.1063/1.4981873

[14] Burrell K H 1999 *Physics of Plasmas* **6** 4418–4435 URL https://doi.org/10.1063/1.873728

[15] Boedo J A *et al.* 2021 *Private Communication*

[16] Theiler C, Furno I, Ricci P, Fasoli A, Labit B, Müller S H and Plyushchev G 2009 *Phys. Rev. Lett.* **103**(6) 065001 URL https://link.aps.org/doi/10.1103/PhysRevLett.103.065001

[17] D'Ippolito D A, Myra J R and Zweben S J 2011 *Physics of Plasmas* **18** 060501 URL https://doi.org/10.1063/1.3594609

[18] Myra J R, D'Ippolito D A, Stotler D P, Zweben S J, LeBlanc

B P, Menard J E, Maqueda R J and Boedo J 2006 *Physics of Plasmas* **13** 092509 URL https://doi.org/10.1063/1.2355668

[19] Furno I, Labit B, Podestà M, Fasoli A, Müller S H, Poli F M, Ricci P, Theiler C, Brunner S, Diallo A and Graves J 2008 *Phys. Rev. Lett.* **100**(5) 055004 URL https://link.aps.org/doi/10.1103/PhysRevLett.100.055004